Modeling of Magnetic Saturation in Battery Charger Power Electronics

Dr. Kasemsan Siri and Mr. Michael Willhoff
Electronics and Power Systems Department
April 19 - 22, 2021

Identifying Magnetic Saturation as a Threat

- Each battery charger contains a gate-drive transformer that communicates PWM control signals to the main MOSFETs
- This push-pull transformer lacked a mechanism to resist magnetic flux walking
  - *Residual DC voltage appeared across the primary (no capacitive blocking)*
- A sub-harmonic oscillation initiated magnetic flux walking by making the on-time of one phase longer than the other
- Magnetic saturation leads to loss of normal closed-loop battery charge current control
  - *Battery current oscillates at a frequency range from 100 Hz to 5 kHz of oscillation*
  - *The contractors verified and accepted this Aerospace finding*

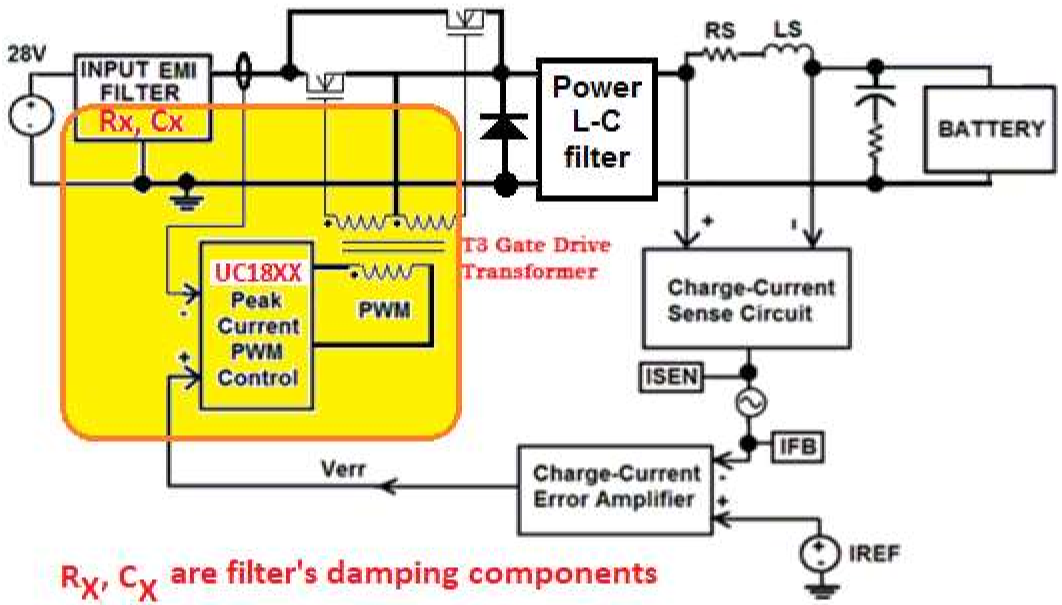

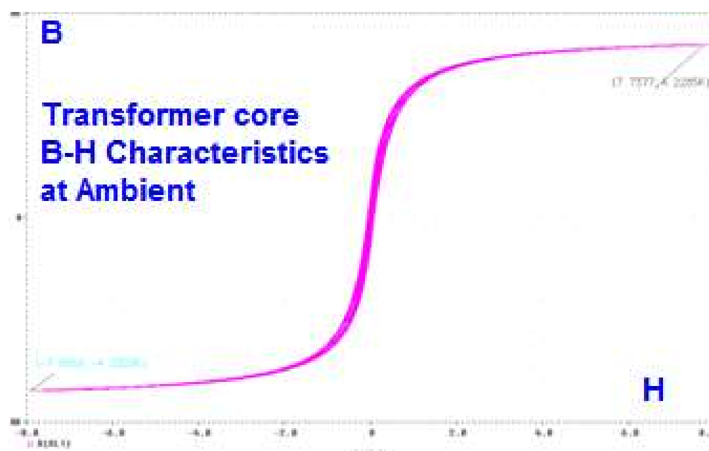

PWM: Pulse Width Modulator, MOSFET: Metal Oxide Field Effect Transistor

Outline of Magnetic Saturation Modeling

- Present an intermediate modeling approach for both linear and non-linear magnetic components.
- The magnetic components can be two-terminal inductors, multiple-terminal coupled inductors, or transformers.
- Discuss basic characteristics of magnetic core materials, revealing the core flux density as a function of the magnetic field strength that is linearly proportional to the current flowing in the magnetic component.
- Provide decomposition of the non-linear magnetic components into the separately interconnected models of linear and non-linear magnetic models.
- Through proper mathematical derivations, exemplify how the linear and non-linear models are related to the original set of Maxwell's equations.
- Extend those mathematics into interconnected PSPICE models that can be used together for simulation of the circuit responses involving the non-linear behavior of these magnetic components.

Top-Level Modeling Diagram of PWM Switch with Saturable Transformer

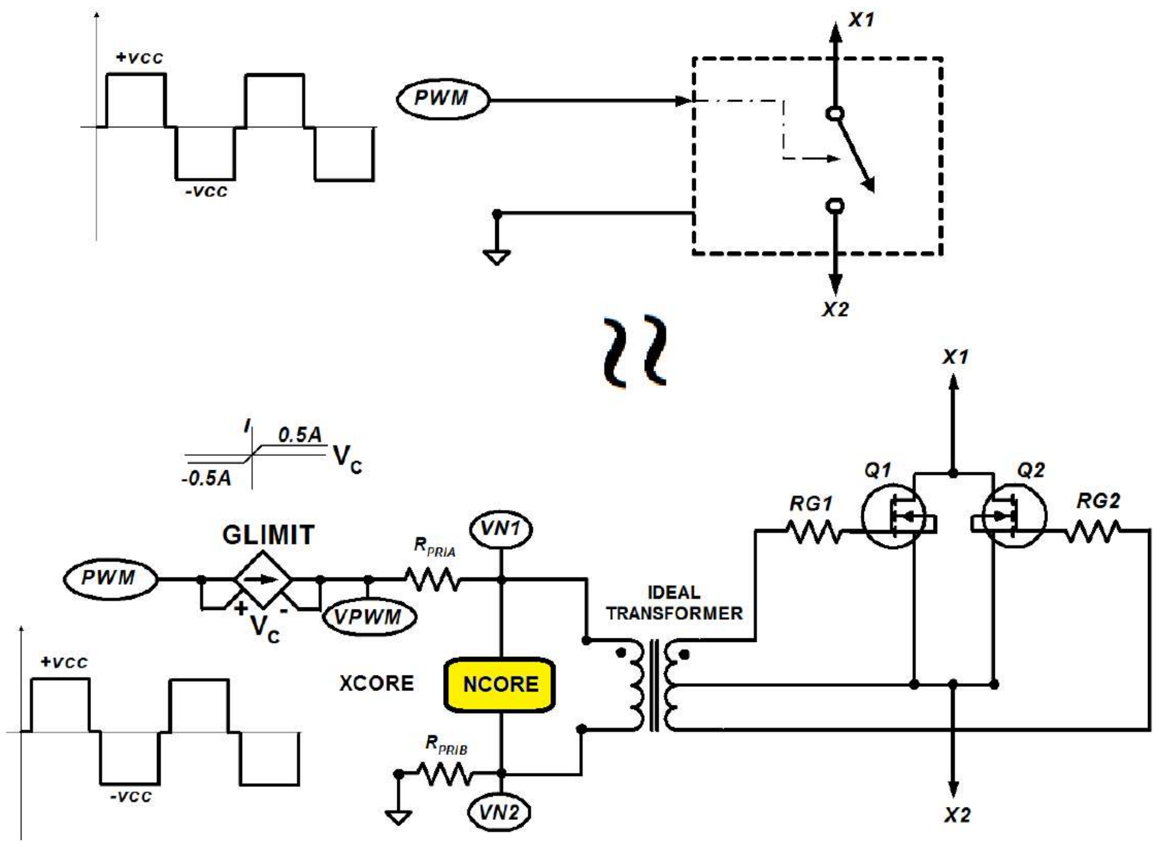

Saturable pulse transformer is decomposed into

– *a non-linear device NCORE and an ideal transformer*

Fundamental Equations for Magnetic Components

- **KVL's Law for inductor voltage:**

$$V_L = L \ \partial I / \partial t$$

- **Faraday's Law for Back EMF (ε):**

$$\varepsilon = - N \ \partial \phi / \partial t$$

- **Ampere's Law:**

$$\oint H \, \partial l = N I$$

- **Where** N = number of conductor turns
  H = magnetizing force in A-T/meter
  I = current in Amperes
  L = winding inductance in Henries
  t = time in seconds,
  ϕ = magnetic flux = B * Ac
  B = flux density in Tesla,
  Ac = core area in m^2
  V_L = induced voltage in volts across the winding
  l_m = magnetic path length in meters

Scaling both X and Y Axes

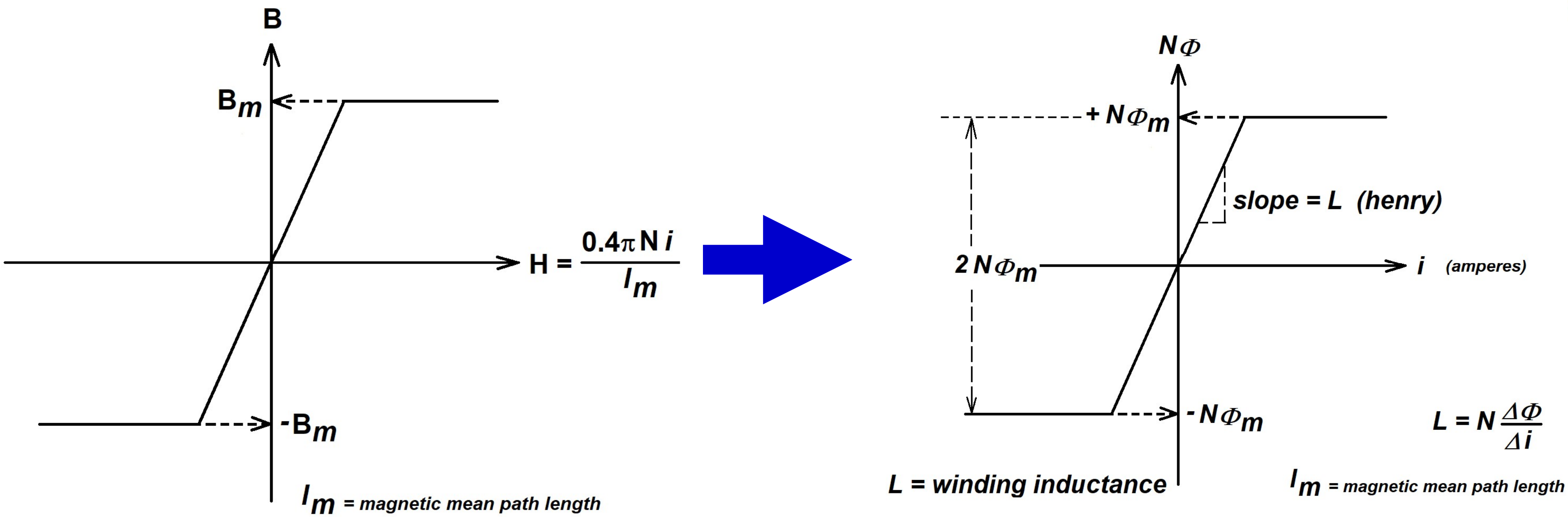

$I = H / k1$ where $k1 = N*\pi / l_m$, l_m = magnetic path length

$N\,\Phi = B * k2$ where $k2 = N*Ac$, Ac = cross-section core area

Normalization

Flux linkage (NΦ) is converted to normalized flux ($flux_n$)

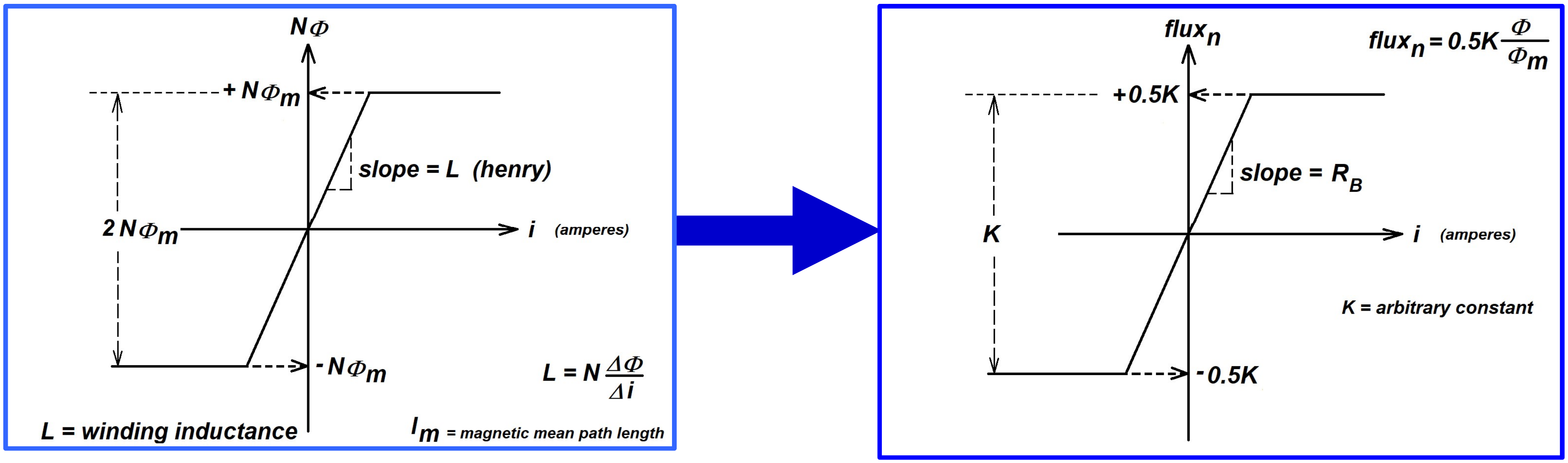

Vertical-axis normalized factor = K/(2*N*Φ_m)

Where Φm = saturation magnetic flux = Bm*Ac

Normalized Flux Equation

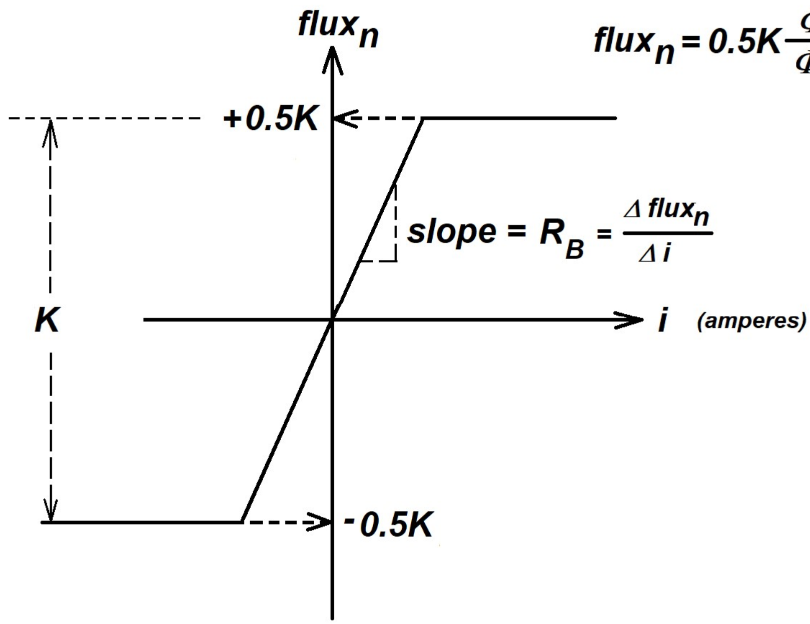

$$flux_n = 0.5K \frac{\Phi}{\Phi m}$$

$$N \frac{d\Phi}{dt} = V_L$$

$$N\Phi = \int_0^t V_L\, dt$$

K = arbitrary constant

K = 500

Normalized factor of $\frac{2N\Phi m}{K}$

$$\boxed{flux_n = \frac{K}{2N\Phi m} \int_0^t V_L\, dt}$$

V_L = voltage across the electrical winding having *N* turns of conductive wire wrapping around the magnetic core material

K = arbitrary factor (preferred value of 500 or greater)

$flux_n$ = normalized flux saturated at +/- 0.5*K

Slope R_B is proportional to permeability (μ) or inductance (L)

Mathematical Integration Using Basic Circuit Models: A Current Source and a Capacitor

$$N\frac{d\Phi}{dt} = V_L$$

$$N\Phi = \int_0^t V_L\,dt$$

K = arbitrary constant

K = 500

Normalized factor of $\frac{2N\Phi m}{K}$

$$\boxed{flux_n = \frac{K}{2N\Phi m}\int_0^t V_L\,dt}$$

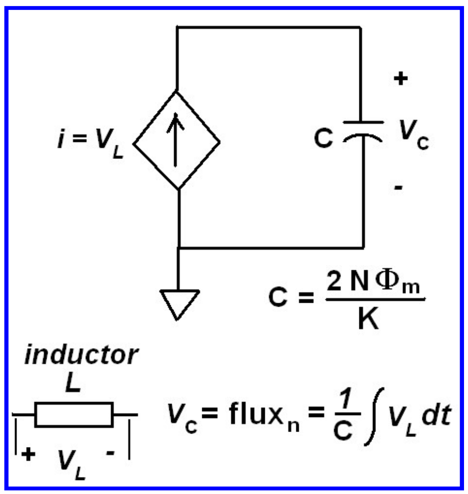

(1) Represent the inductor voltage as a current source

(2) Represent the normalized flux constant as a capacitor

(3) Connected them together to solve for the capacitor voltage response

(4) The capacitor voltage represents the normalized flux ($flux_n$) that is accumulated in the inductor core

$flux_n$ = normalized flux saturated at +/- 0.5*K

Electrical-Magnetic Equivalent Circuit for Simulation of Inductor Current Response

$$\boldsymbol{I} = flux_n / R_B$$

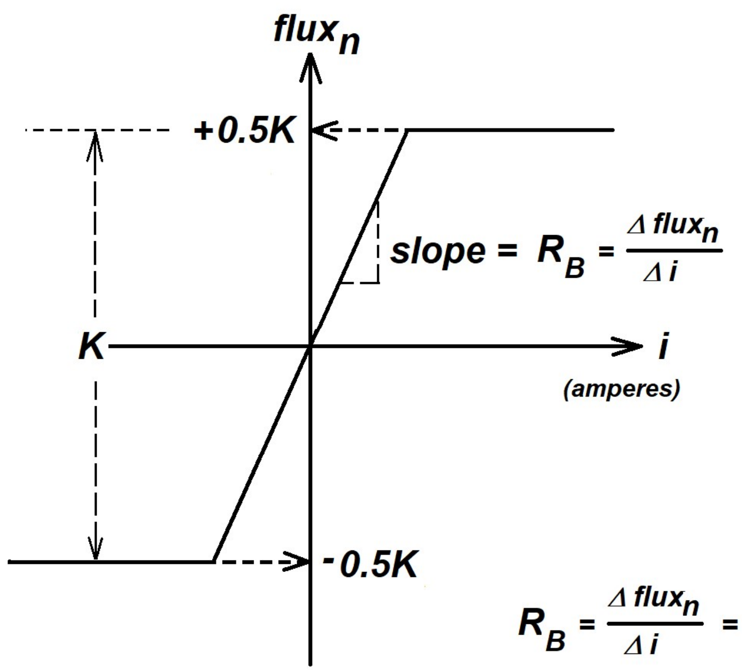

where L = magnetizing inductance before core saturation

$$L = \{LMAG\} = u_0 u_r N^2 \frac{Ae}{l_m}$$

$$L\, i = N\Phi$$

$$i = \frac{N\Phi}{L}$$

$$i = \frac{flux_n}{R_B}$$

$$R_B = \frac{\Delta\, flux_n}{\Delta\, i} = \frac{L \times K}{2\, N\Phi_m} = \frac{K^{*} LMAG}{2\ {}^{*}VSEC^{*}N}$$

where $VSEC = \Phi_m = B_m{}^{*} A_e$

Current = Voltage / Resistance

Electrical-Magnetic Equivalent Circuit for i= $flux_n/R_B$

Current = Voltage / Resistance

(1) ASSIGN THE NORMALIZED MAGNETIC FLUX AS A VOLTAGE SOURCE (V)

(2) DEFINE A RESISTOR, R, AS A FUNCTION OF THE SCALED INDUCTANCE

(3) CONNECT (1) & (2) TOGETHER TO SOLVE FOR THE CURRENT *I*

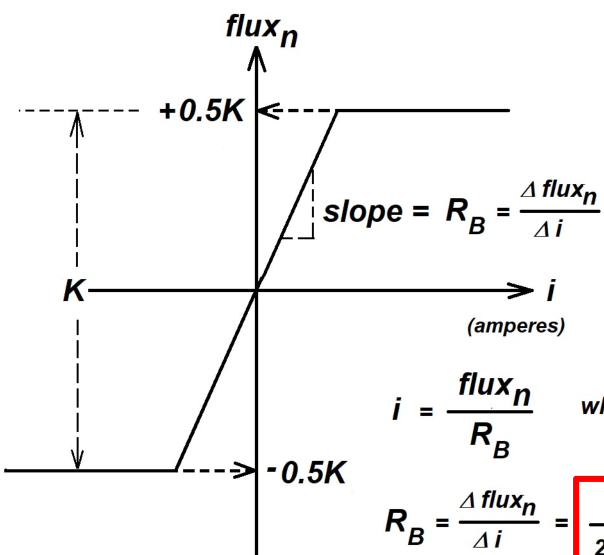

$$i = \frac{flux_n}{R_B} \quad \text{where } VSEC = \Phi_m = B_m * A_e$$

$$R_B = \frac{\Delta\, flux_n}{\Delta i} = \boxed{\frac{L \times K}{2N\Phi_m}} = \frac{K * LMAG}{2 * VSEC * N}$$

Scaled Inductance

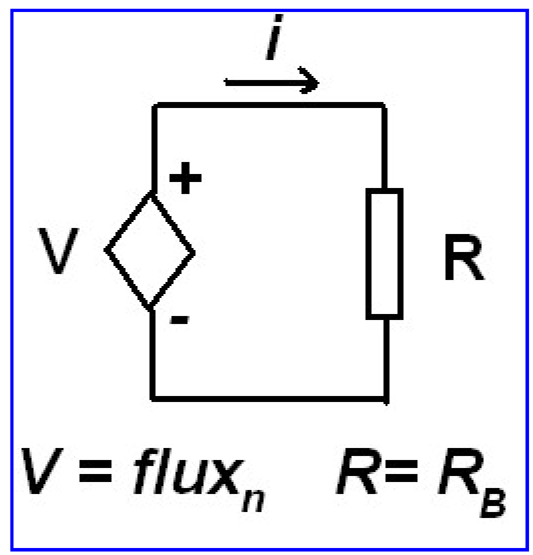

Equivalent Circuit Model for Saturated-Core Inductor (Air-Core Inductor)

(1) REPLACE THE SATURATED-CORE INDUCTOR WITH ANOTHER RESISTOR

(2) REPLACE +/- SATURATED FLUX LEVEL WITH A BI-DIRECTIONAL ZENER DIODE

(3) CONNECT THEM IN SERIES TO SOLVE FOR THE INDUCTOR CURRENT *i*

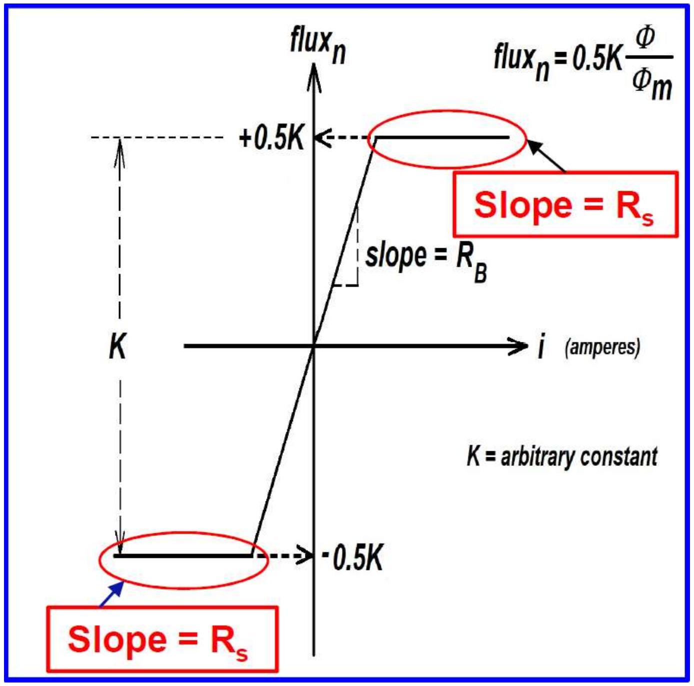

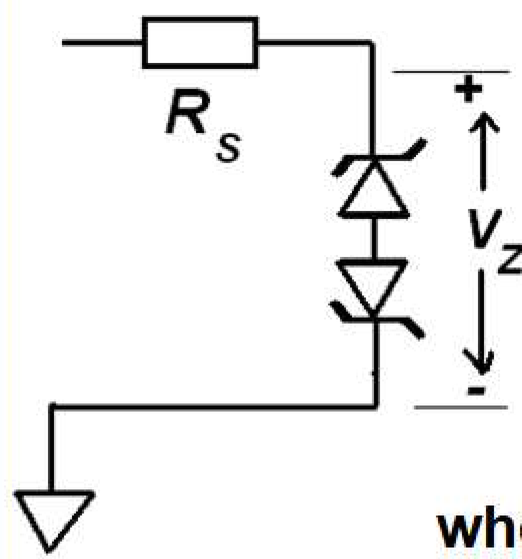

$$R_S \approx L_{SAT} \frac{K}{2N\Phi_m}$$

$$L_{SAT} = u_0 N^2 \frac{Ac}{Lm}$$

$$V_Z = +/- 0.5*K$$

where L >> L_{SAT}

Equivalent Circuit in PSPICE With Air Gap Insertion

$$R_S = \left\{ \frac{L_{SAT} \times K}{2N \times VSEC} \right\} \qquad R_B = \left\{ \frac{L_{MAG} \times K}{2N \times VSEC} \right\}$$

Where $R_G = \dfrac{L_{gap} \times K}{2N \times VSEC}$

$$L_{SAT} = \mu_0 N^2 \frac{A_c}{l_m}$$

$$L_{gap} = u0 \cdot N^2 \cdot \frac{Ac}{lg}$$

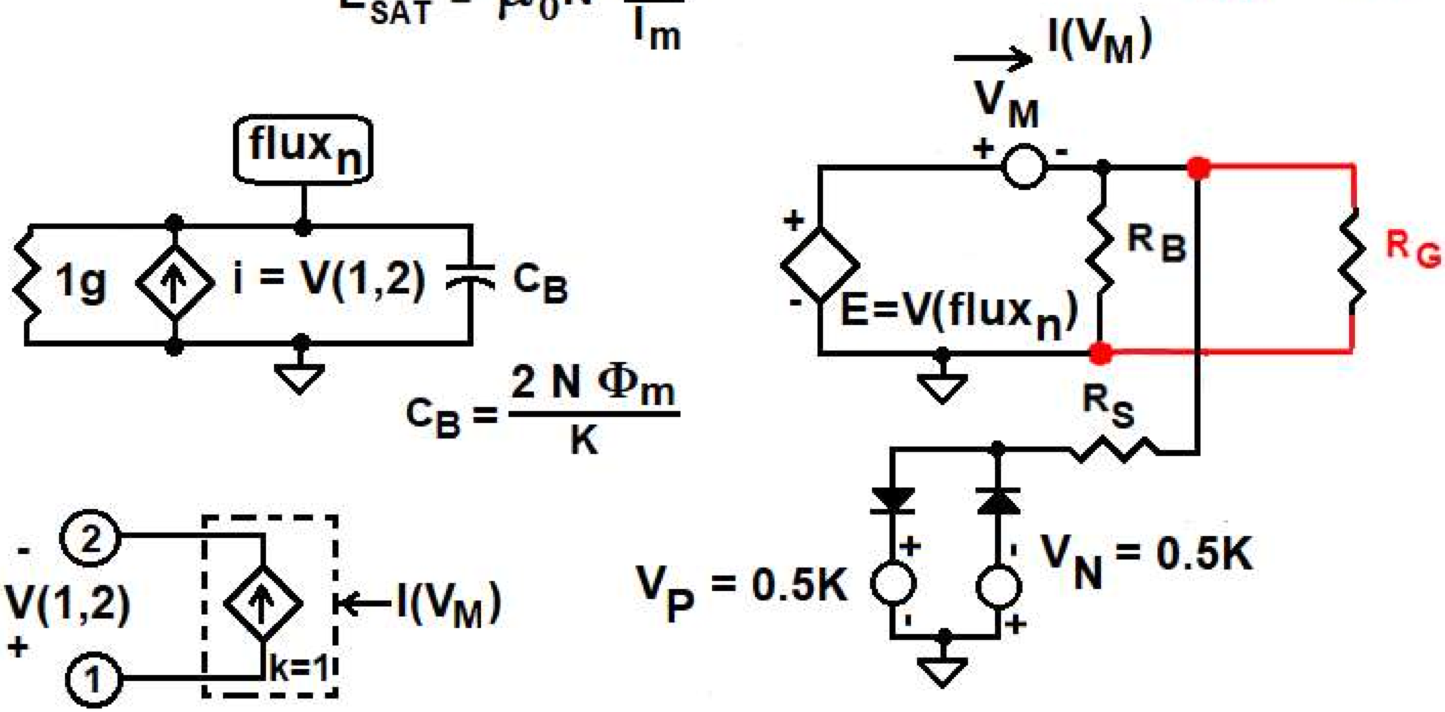

Input Parameters for Equivalent Core Model in PSPICE Schematic

B_m: Saturation flux density in Gauss
A_c : core cross-section area in cm^2
l_m: magnetic path length in cm
N: # of turns
u_r: relative permeability
K in an arbitrary number >> 1 i. e. K =500

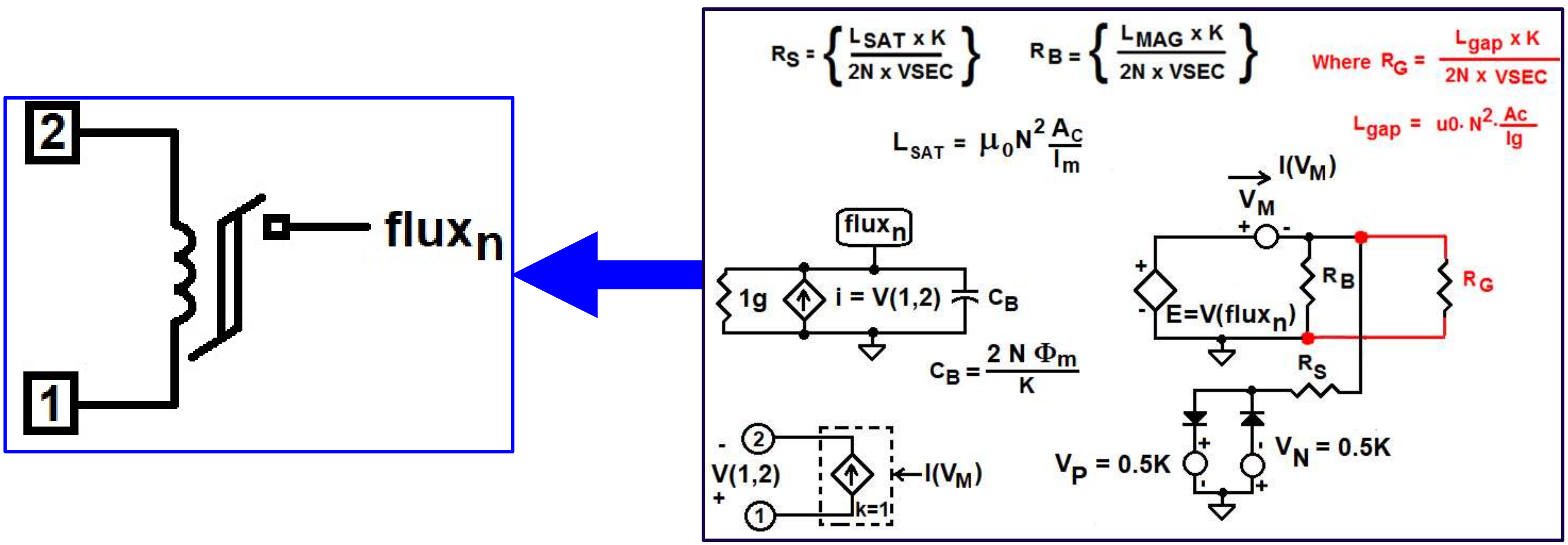

PSPICE Schematic diagram of NCORE Model

$$LMAG = \mu_0 \mu_r N^2 AC/LM \qquad LSAT = \mu_0 N^2 AC/LM \qquad R_G = \frac{L_{gap} \times K}{2N \times SVSEC}$$

$$R_S = \left\{ \frac{L_{SAT} \times K}{2N \times SVSEC} \right\} \qquad R_B = \left\{ \frac{L_{MAG} \times K}{2N \times SVSEC} \right\} \qquad C_B = \frac{2N \times SVSEC}{K} \qquad L_{gap} = u0 \cdot N^2 \cdot \frac{Ac}{lg}$$

$SVSEC = BSAT \times AC$ $\qquad$ $IVSEC = BI \times AC$ $\qquad$ $K = 500$ $\qquad$ $AC = 2$

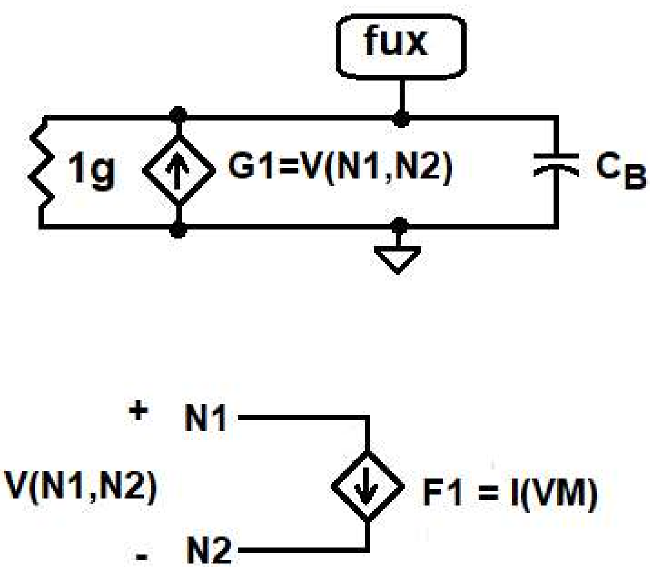

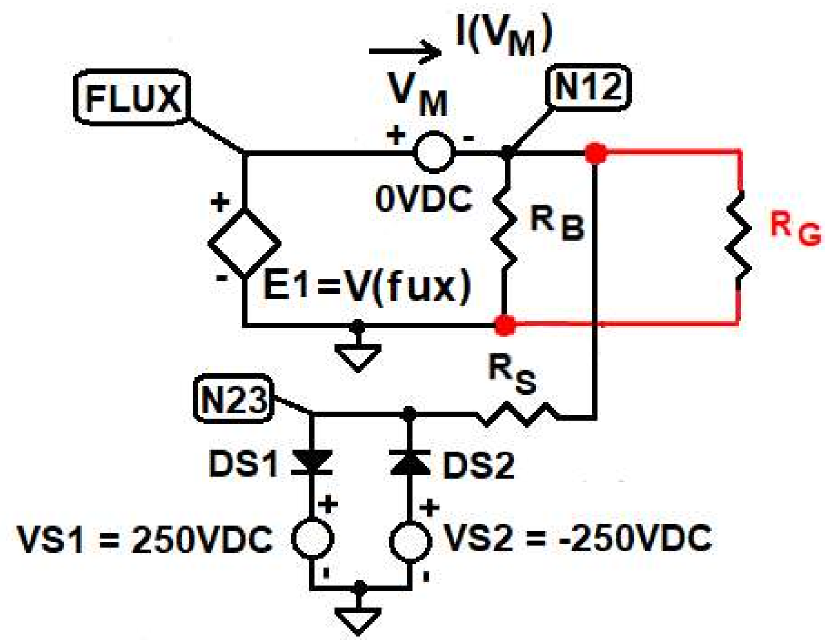

PSPICE NETLIST codes are in the APPENDIX.

Piecewise-Linear Three-Slope Non-Linear Model

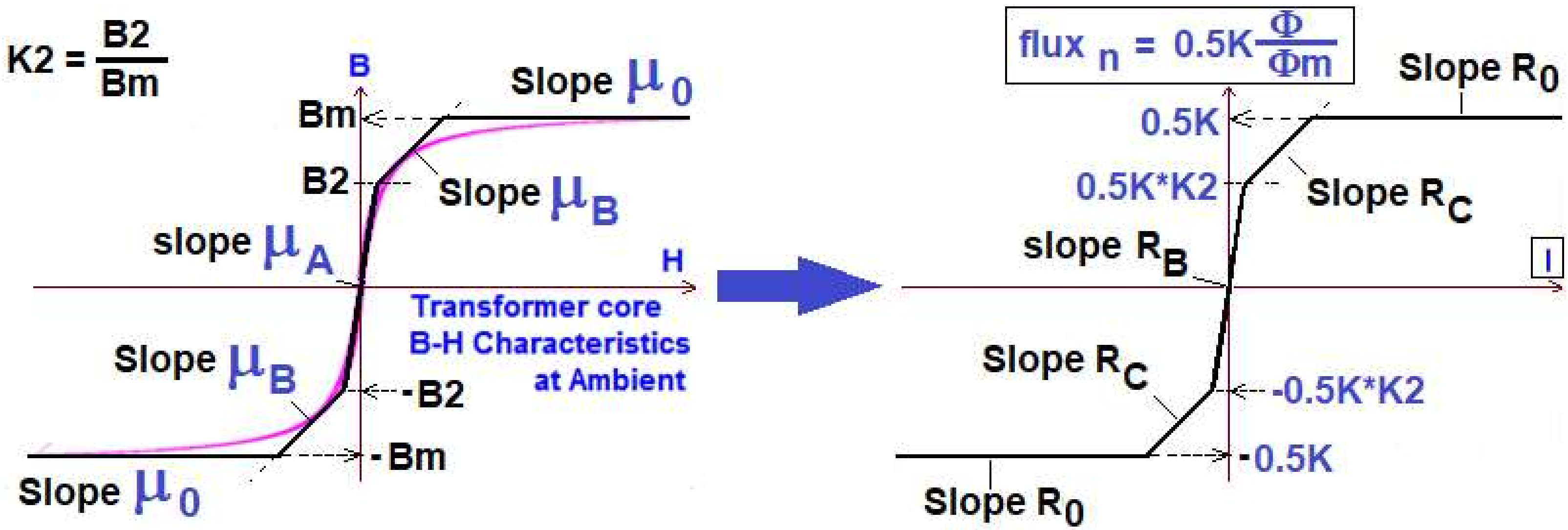

(I) Partitioning B-H curve into three piecewise linear slopes: μA, μB, and μ0

(II) Linearly mapping into three piecewise linear slopes: $\mathbf{R_B}$, $\mathbf{R_C}$, **and** $\mathbf{R_0}$

Piecewise-Linear Three-Slope Non-Linear Model

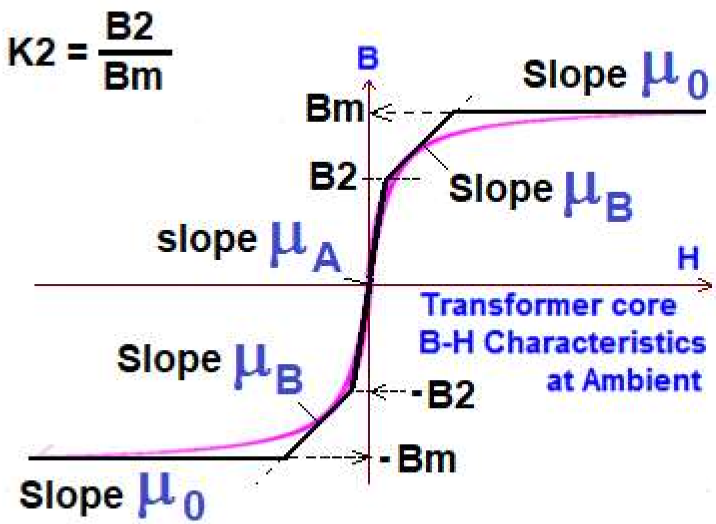

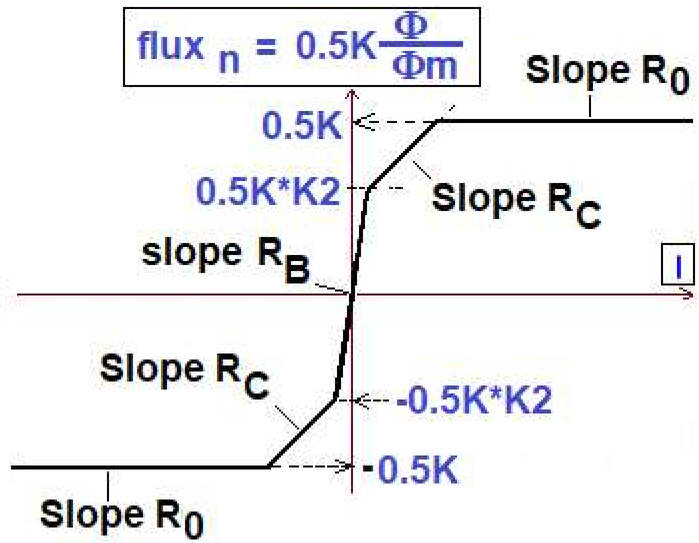

Where slope parameters: $R_B = \alpha\ \mu_A$, $R_C = \alpha\ \mu_B$, $R_0 = \alpha\ \mu_0$

$$\alpha \quad = (0.5K*N*A_C\ ) / (\Phi_m L_m)$$

$\Phi_m = B_m A_{C,}$ A_C = core area, L_m = magnetic path length

Electrical Circuit Equivalent Model

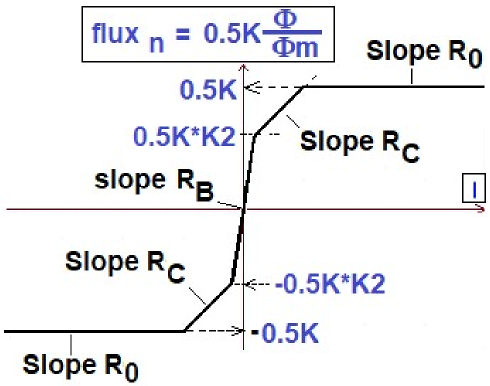

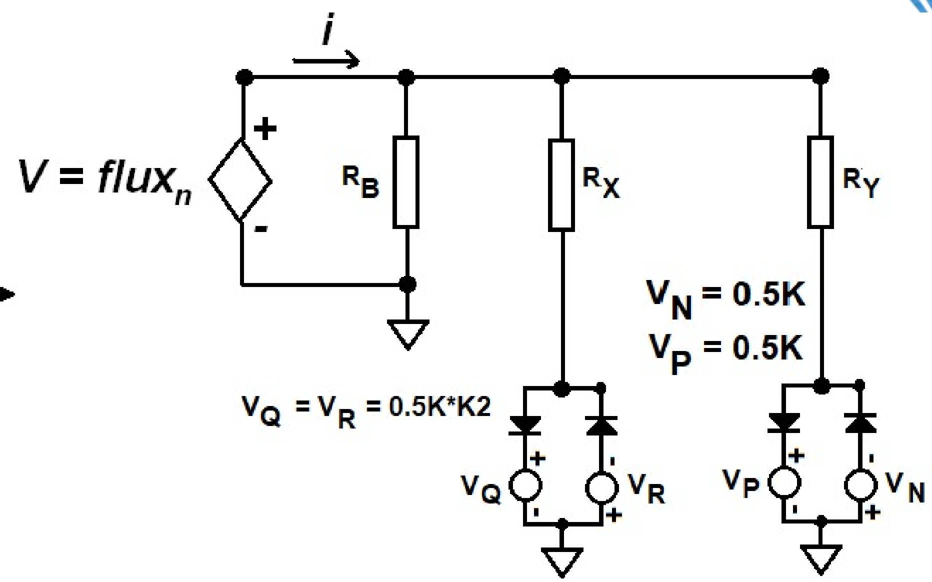

Where $R_C = \frac{R_X R_B}{R_X + R_B}$ $\quad R_0 = \frac{R_Y R_C}{R_Y + R_C}$ $\quad K2 = \frac{B_2}{B_m}$

- 3-Slope Piecewise B-H curve is transformed into an electrical circuit which is used to solve for the inductor current response, ***i***
- R_X is computed from R_B and R_C
- R_Y is computed from R_0 and R_C

Equivalent Transformer Model in PSPICE Schematic

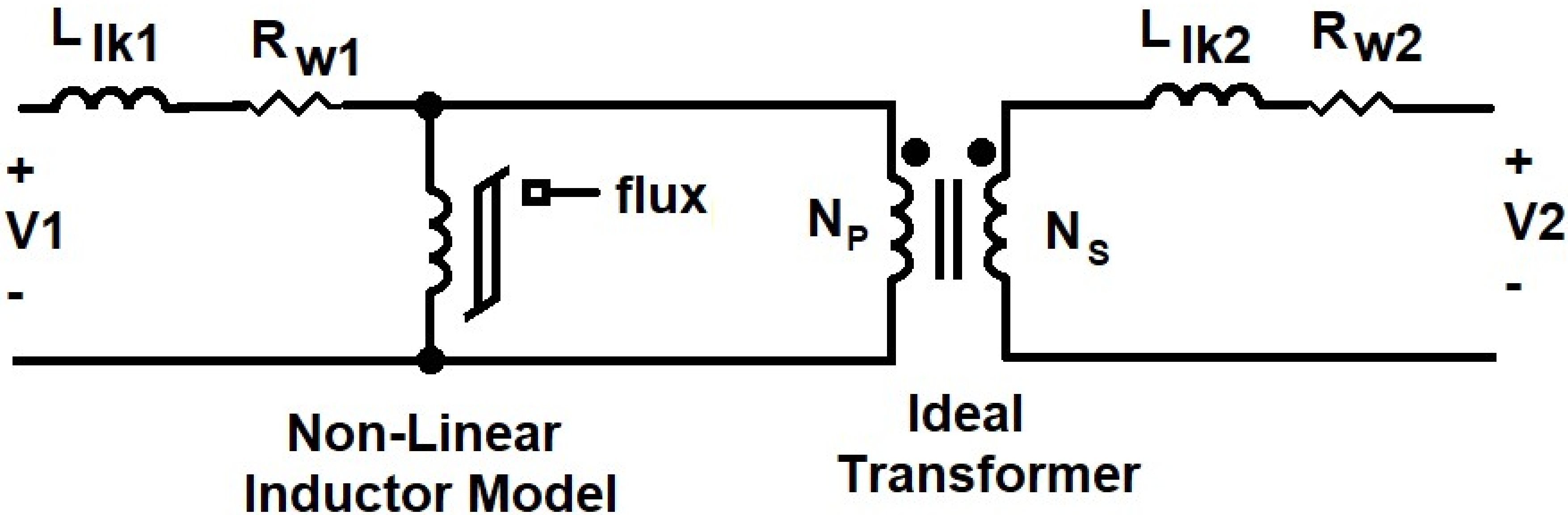

Only one non-linear element contains the magnetic core model. Otherwise, other circuit elements are linear.

Summary

- Analytical details behind modeling of magnetic saturation within an isolation transformer was presented

- The APPENDIX charts for this presentation also include:
  - *The full motivation behind this modeling and analysis effort*
  - *The simulation results that are correlated with test data*
  - *Actual design corrections that eliminate magnetic saturation*
  - *PSPICE netlist codes for the magnetic saturation modeling*

- Introductory presentation on this subject can be found on CD-ROM for Space Power Workshop 2019, under the presentation entitled as “Magnetic Saturation, A Lesson Learned from Battery Charger Power Electronics,” Kasemsan Siri and Michael Willhoff, Electronics and Power Systems Department, April 1 - 4, 2019

Backup (APPENDIX)

Battery Charger Modifications (Design Corrections)

- Battery charger had intermittent output current dropouts
  - *Marginal design had negative timing margins resulting in large signal oscillation*
  - *Generic deficiency: charge-current dropouts also detected on 3 more satellites under test*
  - *Customer and contractor agreed to modify the battery charger under the constraint of re-using the existing printed circuit boards*
- Effort mitigated battery charge current drop-outs & oscillation by:
  - *Lowering the DC charge current to two-third (2/3) of the previous charge current*
  - *Improving PWM control signal timing margins to eliminate PWM Pulse-Skipping (Tentative Subject for SPW 2022)*
  - *Clamping voltage spikes that were outside PWM chip ratings*
  - *Eliminating sub-harmonic battery current oscillation*
  - *Re-compensating control loops*
  - ***Eliminating gate drive transformer core saturation***
- Design verification consisted of:
  - *Engineering data collected from non-flight satellite test bed, including validation test over temperature*
  - *Worst Case Circuit Analysis*
  - *Proto-qual unit level test*

Eliminating Transformer Core Saturation

- Adding a series capacitor with the transformer primary winding to provide auto DC-offset counter-balance voltage that ensures no DC voltage across the primary winding

- Replace the existing transformer core material with the better material with nearly 3 times as much the saturation flux density without changing the transformer geometry and specification of its windings

Conceptual Diagram of Battery Charger Control Loop

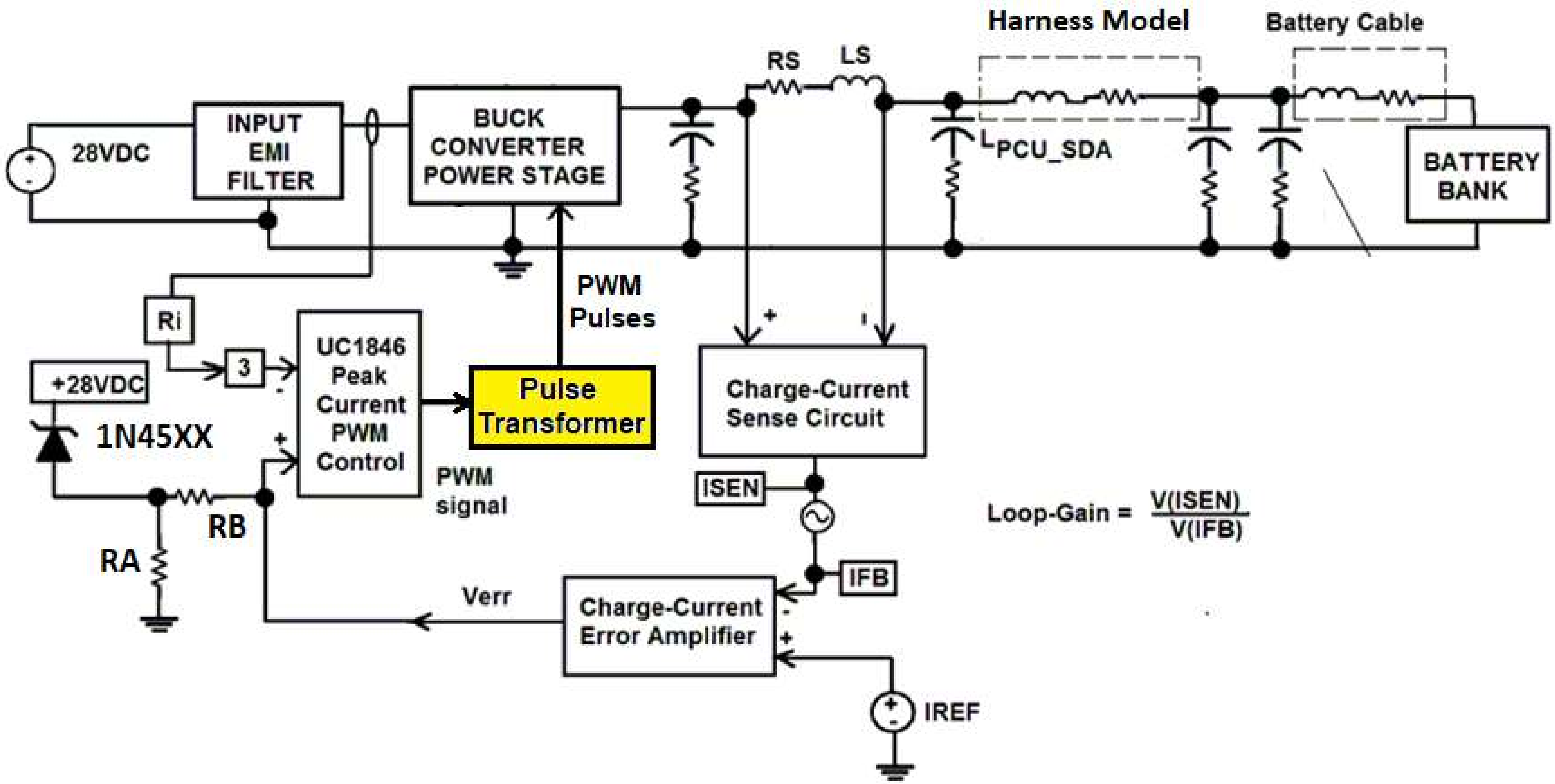

Equivalent Model of Coupled Inductor or Transformer with multiple secondary windings

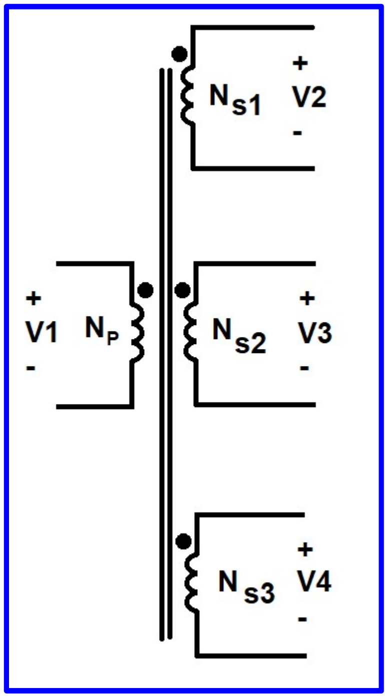

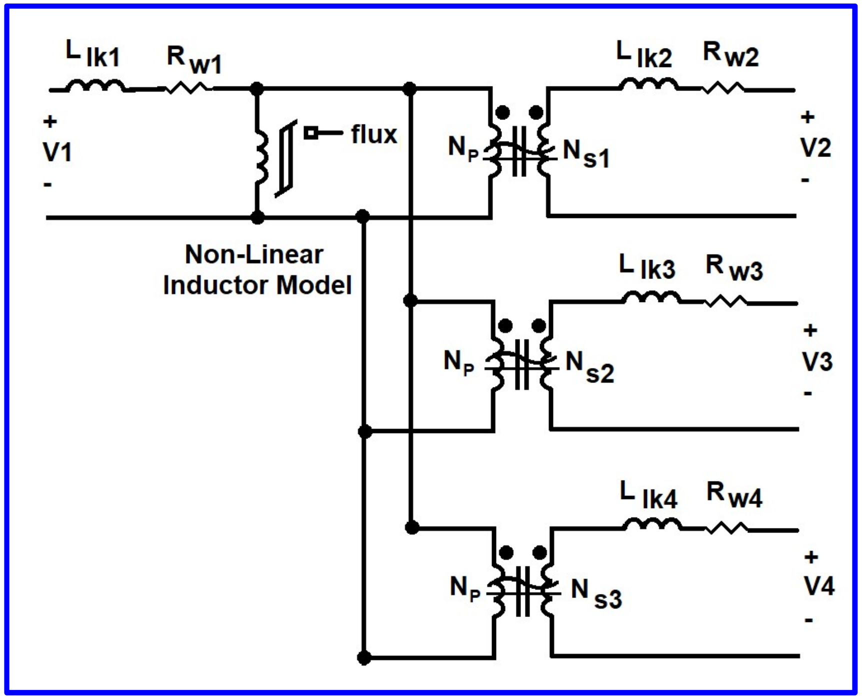

Only one non-linear model is the core model, otherwise other components are linear and ideal.

PSPICE NETLIST OF CORE MODEL (for PSPICE Diagram on Chart 21)

```
*PSPICE NETLIST OF NON-LINEAR
*CORE MODEL WITH HYSTERSIS
.PARAM PI = 3.1415927
.PARAM Bm = XXXX
.PARAM Ac = X
.PARAM Bi = XXX
.PARAM U0 = {4*PI*1E-7}
.PARAM Ur = 100
.PARAM Lm = XX
.PARAM SVSEC = {Bm*Ac}
.PARAM IVSEC = {Bi*Ac}
.PARAM N = X
.PARAM K = 500
.PARAM LMAG = {U0*Ur*Ac*N*N/Lm}
.PARAM LSAT = {U0*Ac*N*N/Lm}
.PARAM Lg = 0.1987
.PARAM Lgap = {U0*Ac*N*N/Lg}
*
***    PAGE 1    ***
```

```
*NON-LINEAR CORE MODEL WITHOUT HYSTERSIS
.SUBCKT  NCORE N1  N2 FLUX
*
G1  0  FUX  N1  N2    1
E1 FLUX   0    VALUE = { V(FUX)}
F1  N1    N2   VM     1
CB FUX   0     {2*SVSEC*N/K} IC = {0.5*K*IVSEC/SVSEC}
VM FLUX   N12   DC=0
RB N12      0          {LMAG*K/(2*SVSEC*N)}
RS N12     N23       {LSAT*K/(2*SVSEC*N)}
RG N12     0          {Lgap*K/(2*SVSEC*N)}
DS2 N22  N23  DCLAMP
DS1 N23  N4    DCLAMP
R3   FUX   0     1G
ES2 N22   0    VALUE= {-0.5*K}
ES1  N4    0    VALUE={0.5*K}
.MODEL DCLAMP D
.ENDS
***              PAGE 2                ***
```

Adding Hysteresis Effect into the Core Model

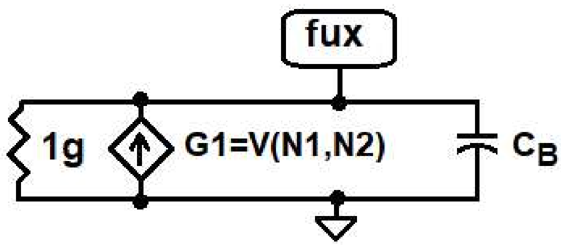

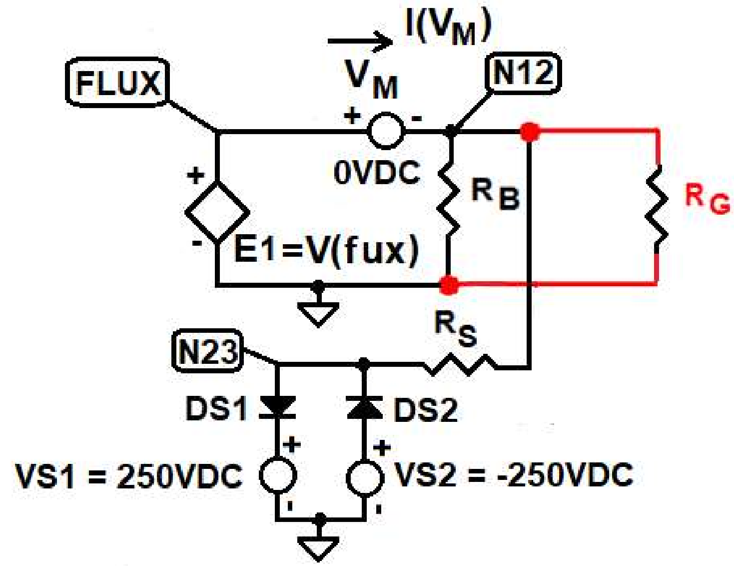

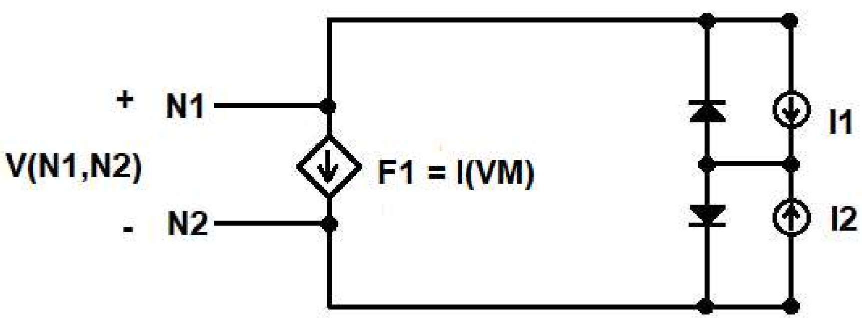

$I1 = I2 = i_O = H0xLM/N$

$K = 500$

Magnetic Saturation Simulation Study

- Motivations:
  - *SV0's time-domain test data reveals sub-harmonics switching in one battery charger, signifying that the charger's pulse transformer experiences asymmetrical driving voltage that possesses significant DC component*
  - *SV0's frequency-domain test data reveals prominent peaks of magnitude and phase of the charger output impedance at sub-harmonic switching frequency (one half of charger's switching frequency)*
  - *More anomaly test data (from two other SVs) reveal the abnormal charge current significantly below the target value*
  - *Without magnetic saturation effects, previous Aerospace simulation (with ideal magnetic components) exhibits no sub-harmonics switching while SV0's test data reveals the sub-harmonic oscillation which further promotes magnetic saturation*
  - *The initial disagreement between the early-phase simulation and the later-phase anomalous test data prompted The Aerospace to include the magnetic saturation effects into the battery charger closed-loop model*

SV = Space Vehicle or a Satellite

Three Possible Levels of Magnetic Saturation

- Benign saturation
  - *Occurs at lower core temperature and its effect is unobservable (no truncation of pulse-width of transformer output voltage)*
- Medium saturation
  - *Occurs at medium core temperature and its effect is observable with sporadic negative spikes in battery charge current (sporadic truncation of PWM pulse)*
- Deep saturation
  - *Occurs at high core temperature and its effect is observable with charge current significantly dropped below its target charge rate (12 A) (truncation of PWM pulse at fundamental switching frequency)*

Gate-Drive Signal from Benign Magnetic Saturation (or no saturation)

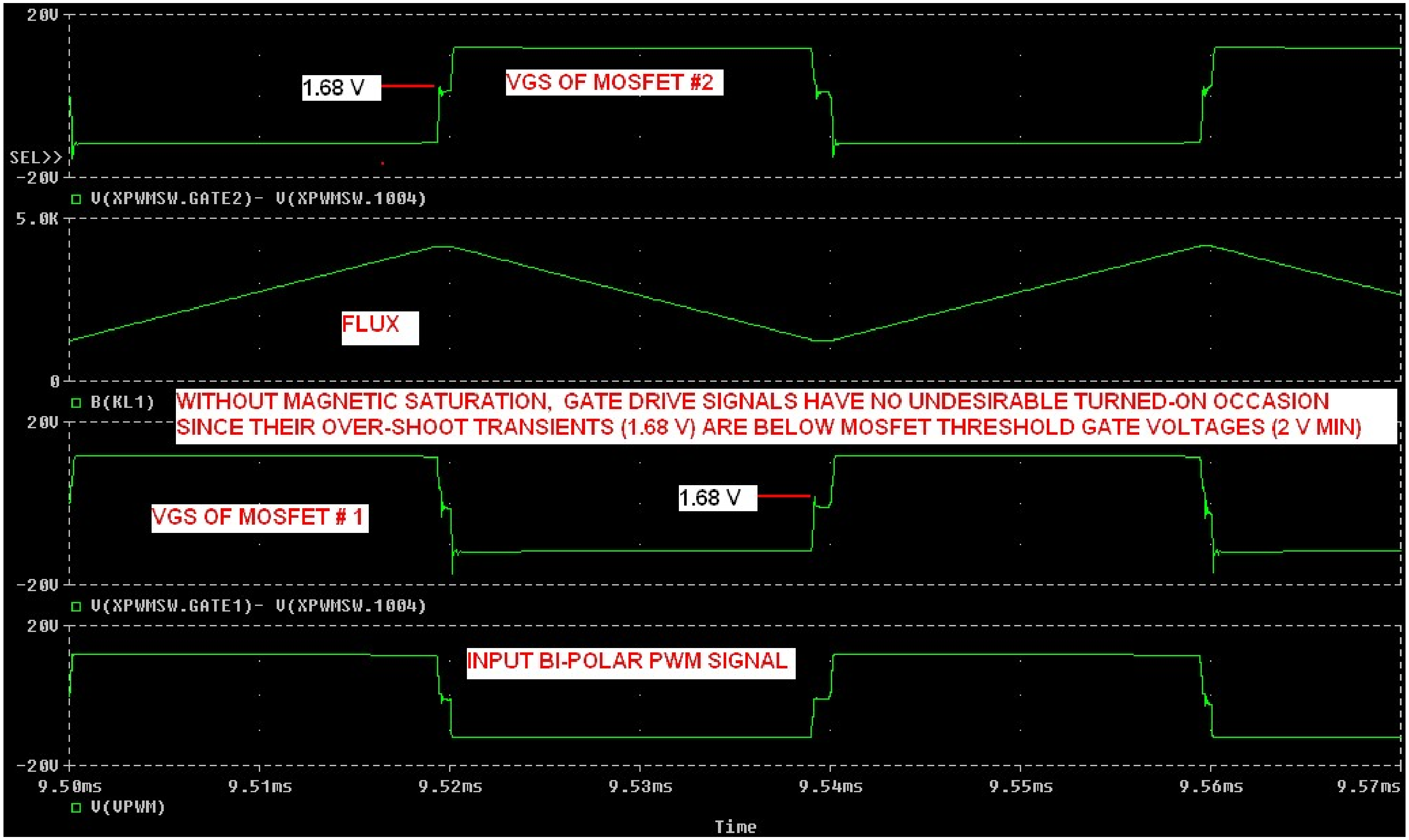

Gate-Drive Signal from Pulse Transformer with Deep Magnetic Saturation

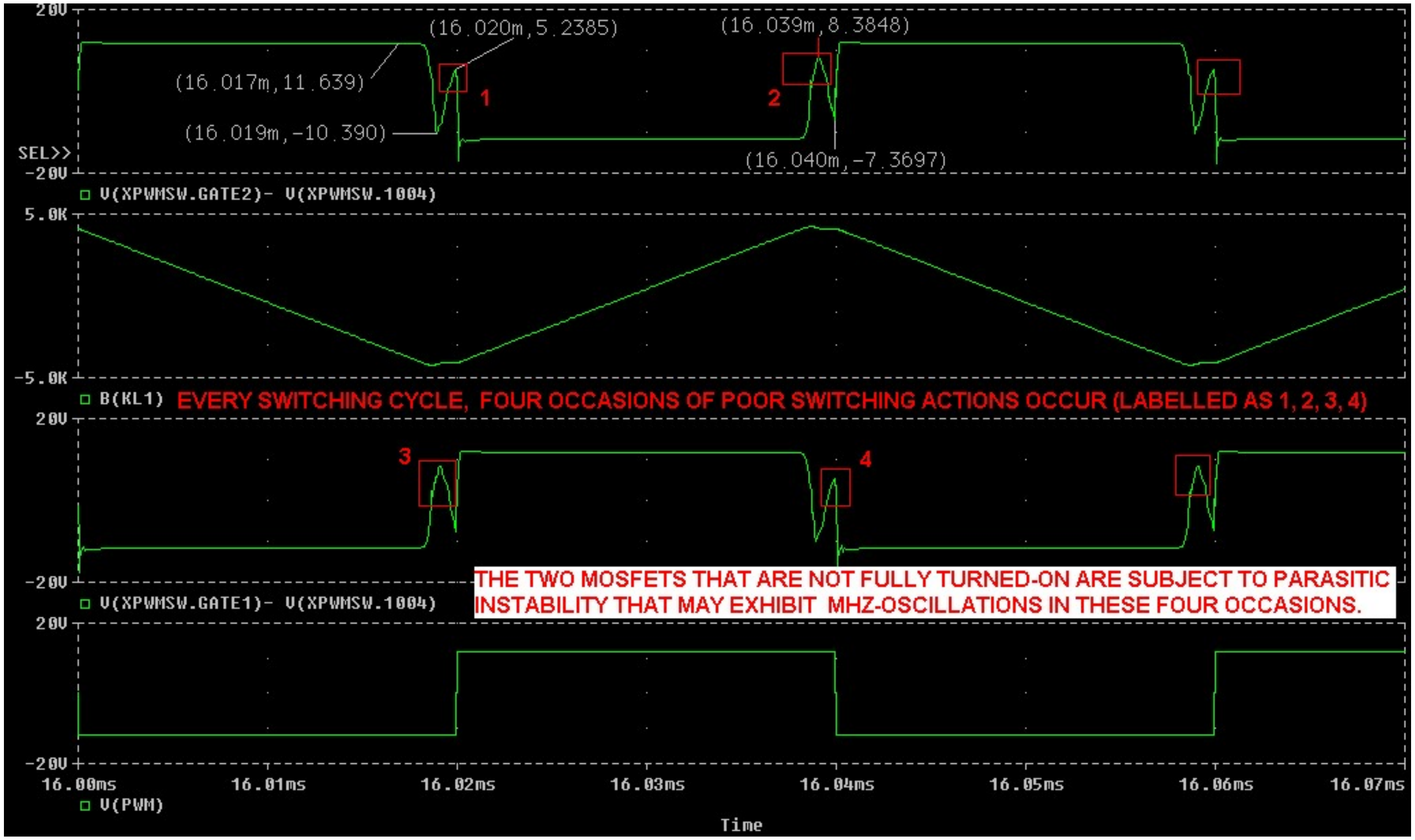

Gate-Drive Signal from Pulse Transformer with Deep Magnetic Saturation (continued)

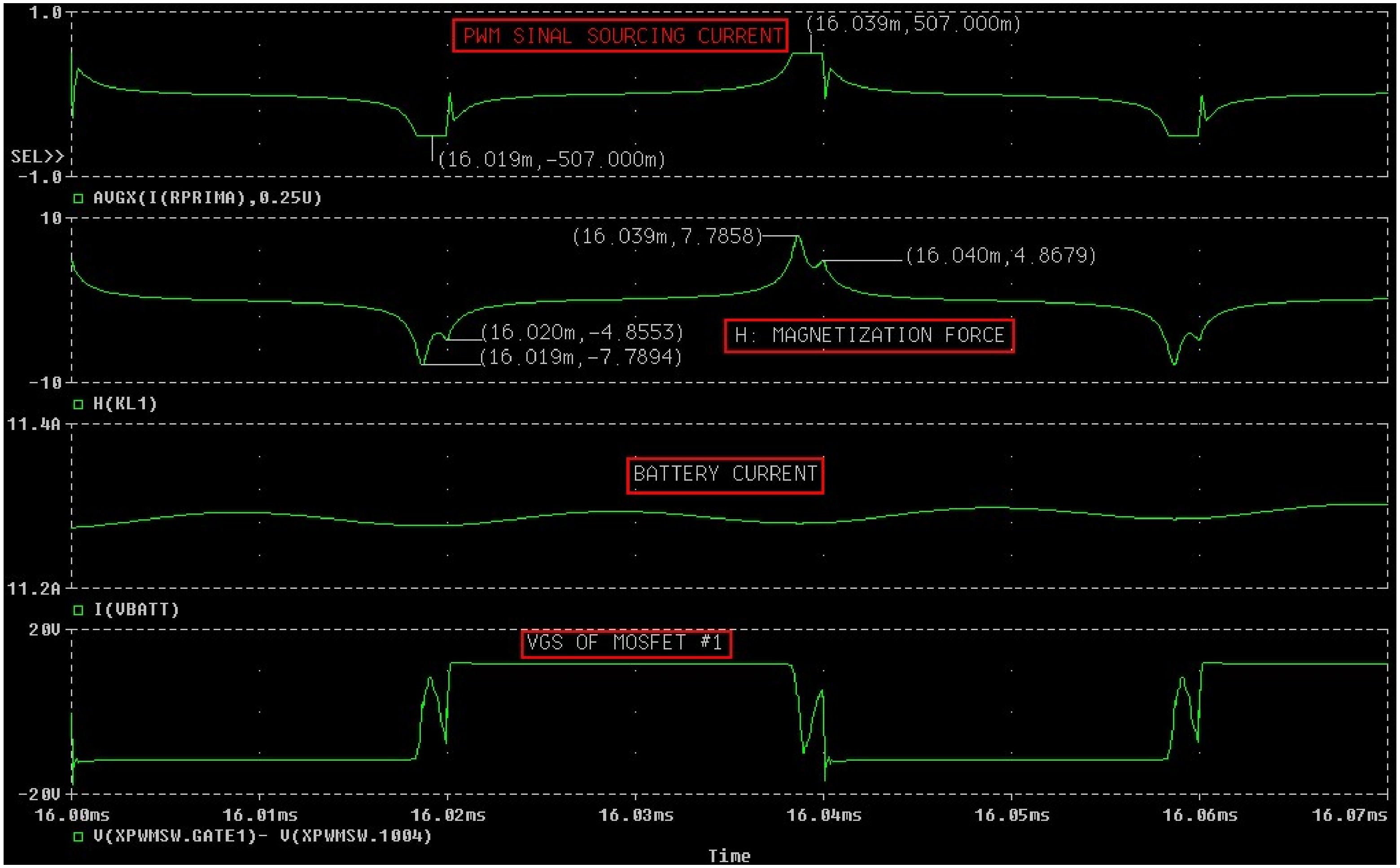

End Result of Deep Magnetic Saturation Charger Control Loop Oscillation

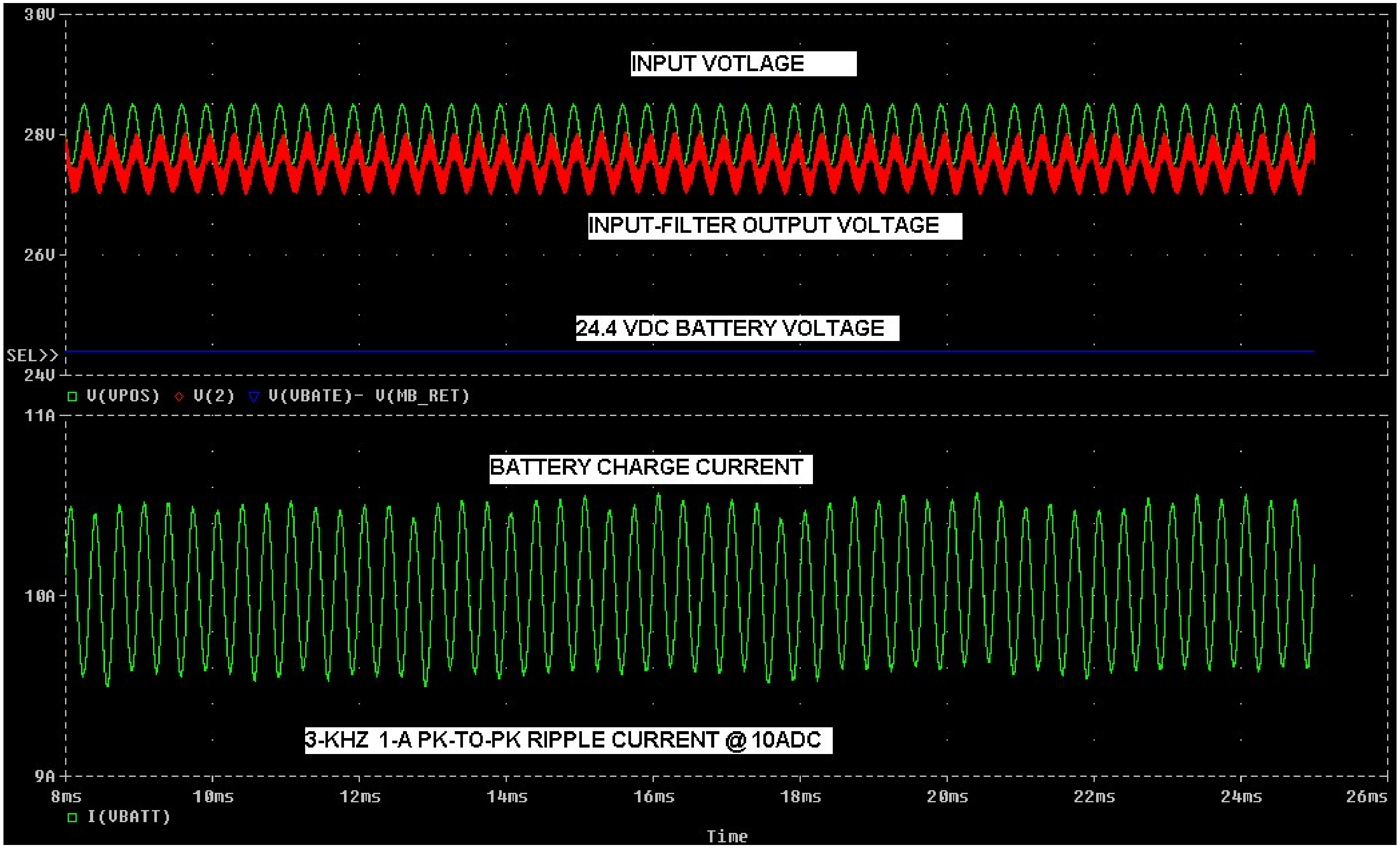

Oscillation @ 3kHz was actually observed from the contractor SV's test data

Conceptual Transformer Output Responses Without Magnetic Saturation VS with Magnetic Saturation

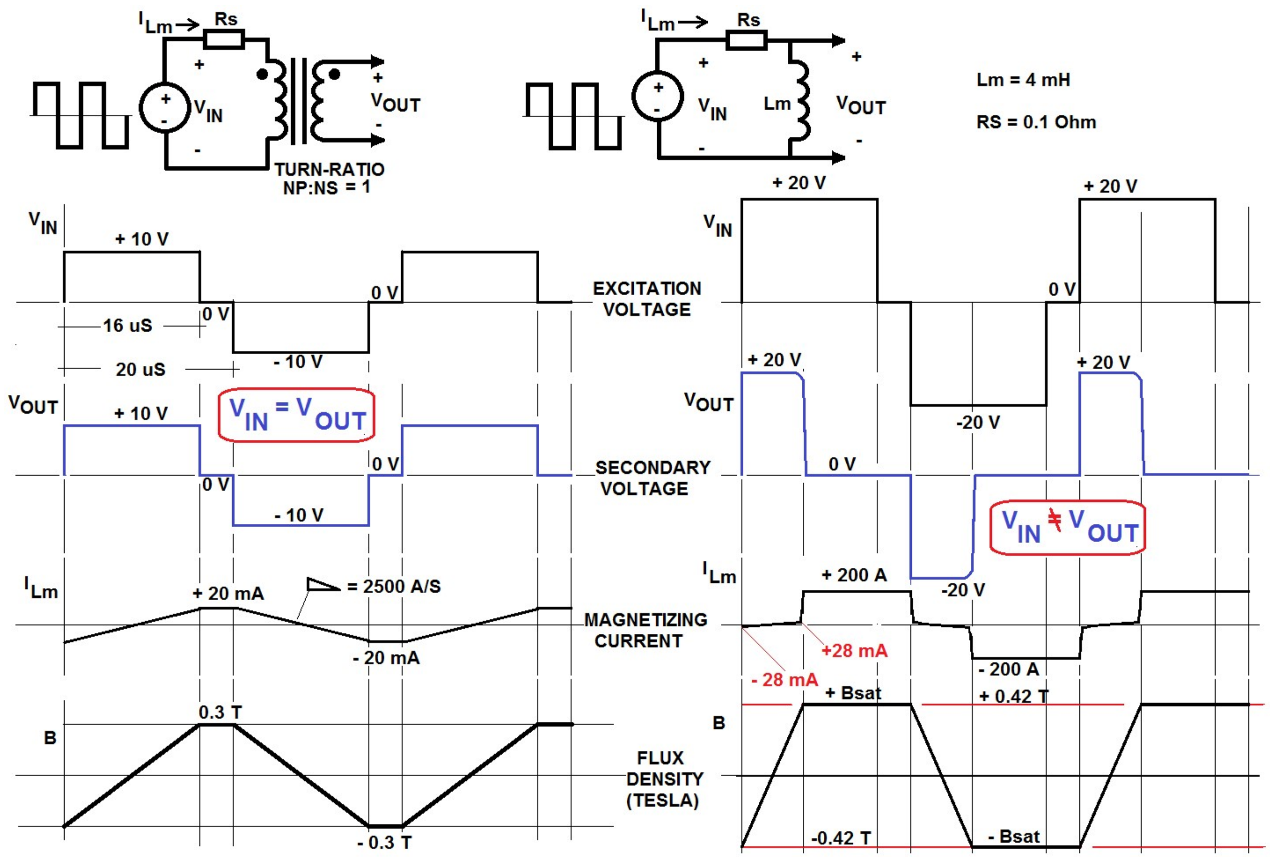

- Typical response of transformer output voltage without magnetic saturation (waveforms on the left) and that with magnetic saturation (on the right)

REFERENCES (internal to Aerospace only)

- “Battery Charger Stability,” K. Siri, 08/06/2008
- “Battery Discharger Stability,” K. Siri, 11/17/2008
- “Power System Stability,” K. Siri, 12/10/2008
- “Effect of RMU Switching Heaters on System Bus Voltage Performance,” K. Siri, 02/09/2009
- “Stability During Overlapping Modes of Operation,” K. Siri, R. Weiss, and D. Tran, 05/09/2011
- “SV05 Risk Assessment,” L. Bell, 04/04/2013
- “Excessive Output Current Identified from Redesigned Battery Charger,” K. Siri, 5/14/2013
- “Conversion of Physical Magnetic Components into Their Equivalent Circuits”, K Siri, 5/17/2013
- “Modeling of Pulse-Skipping in Battery Charger,” K. Siri, 02/15/2013

Thermal Run-Away Behavior due to Proximity of Four Components

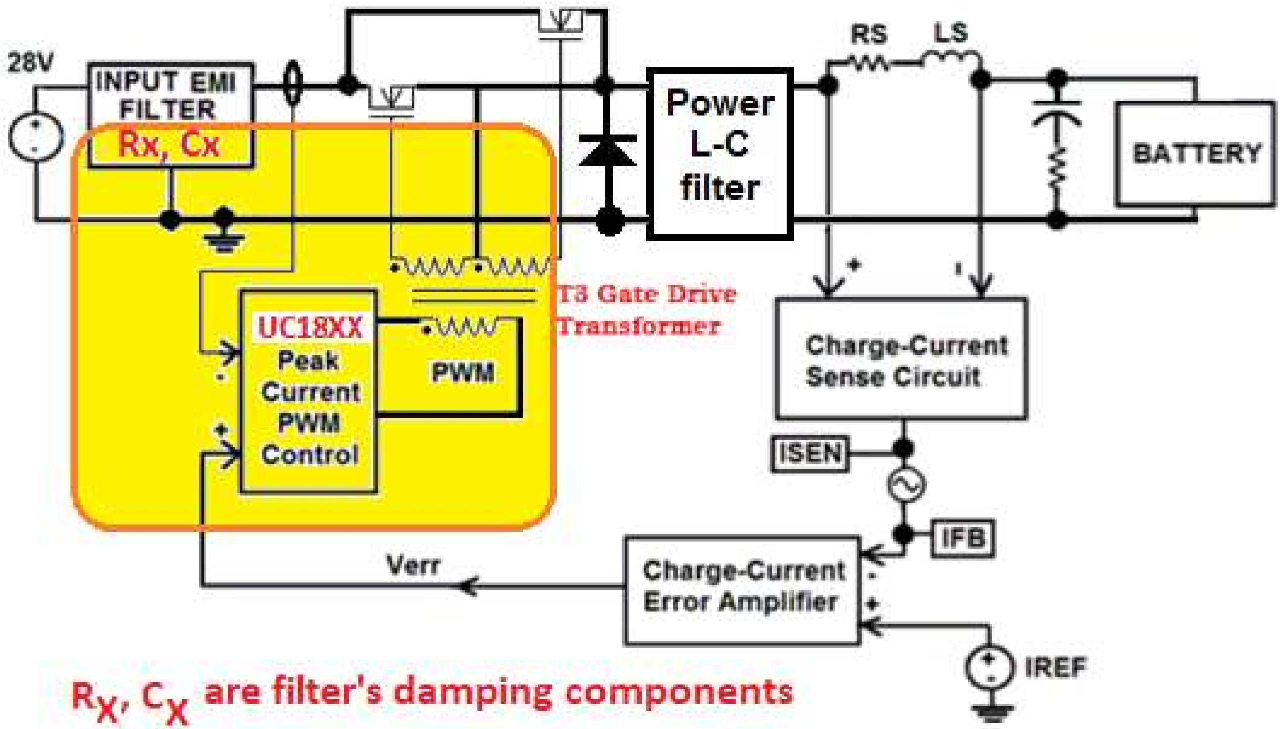

- Heat introduced by the EMI filter damping components (**R_X** & **C_X**) and the PWM chip (UC18XX) creates the positive feedback effect, forcing the heated PWM chip to reduce the switching frequency which further promotes the deeper magnetic saturation in transformer T3. The deeper transformer saturation causes more heat dissipation to the PMW chip, leading to a thermal run-away behavior.

Normal Response without Saturation

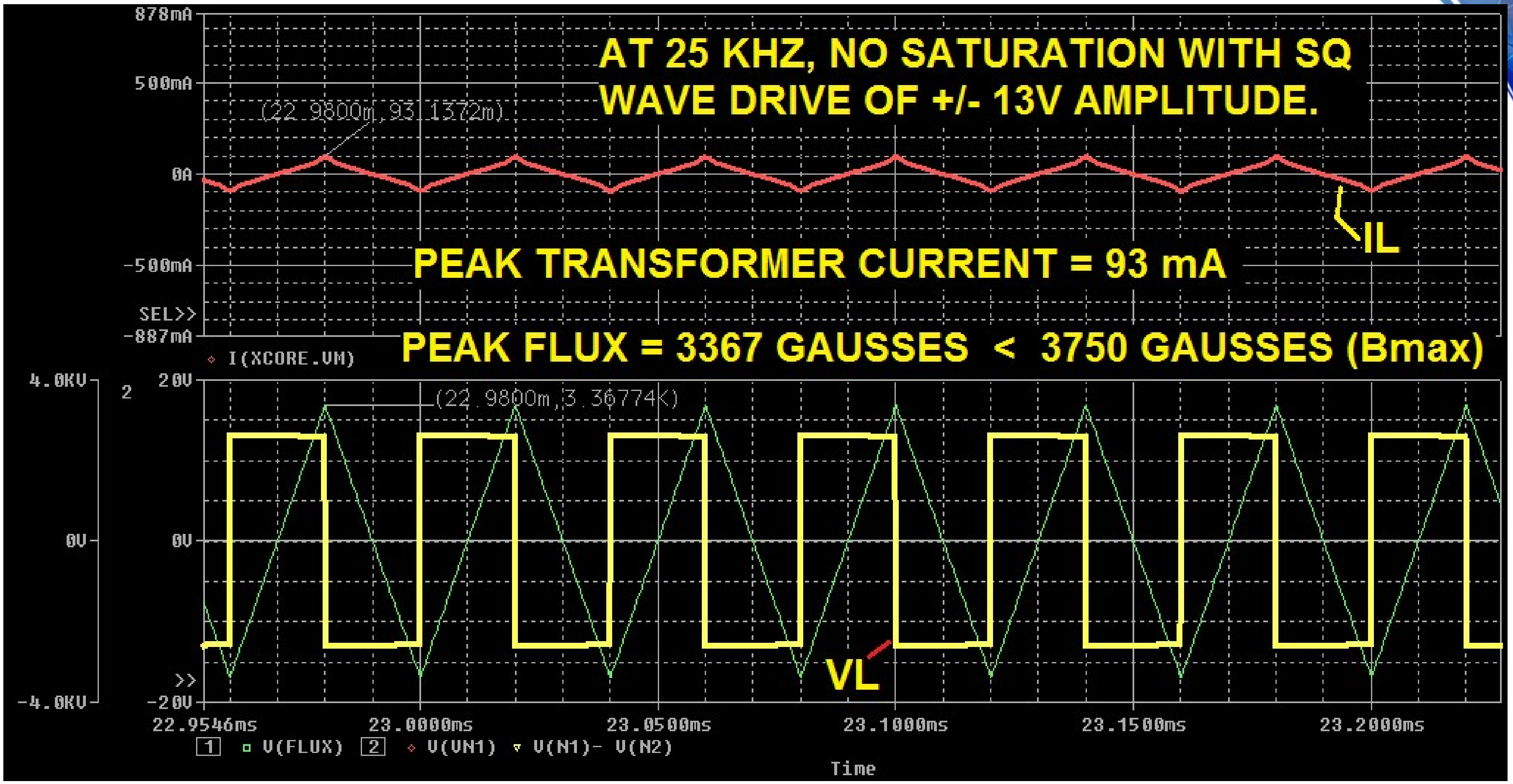

- Normal response occurs at the designed PWM frequency (50 kHz) or the operating transformer frequency of 25 kHz

Gentle Creeping into Magnetic Saturation

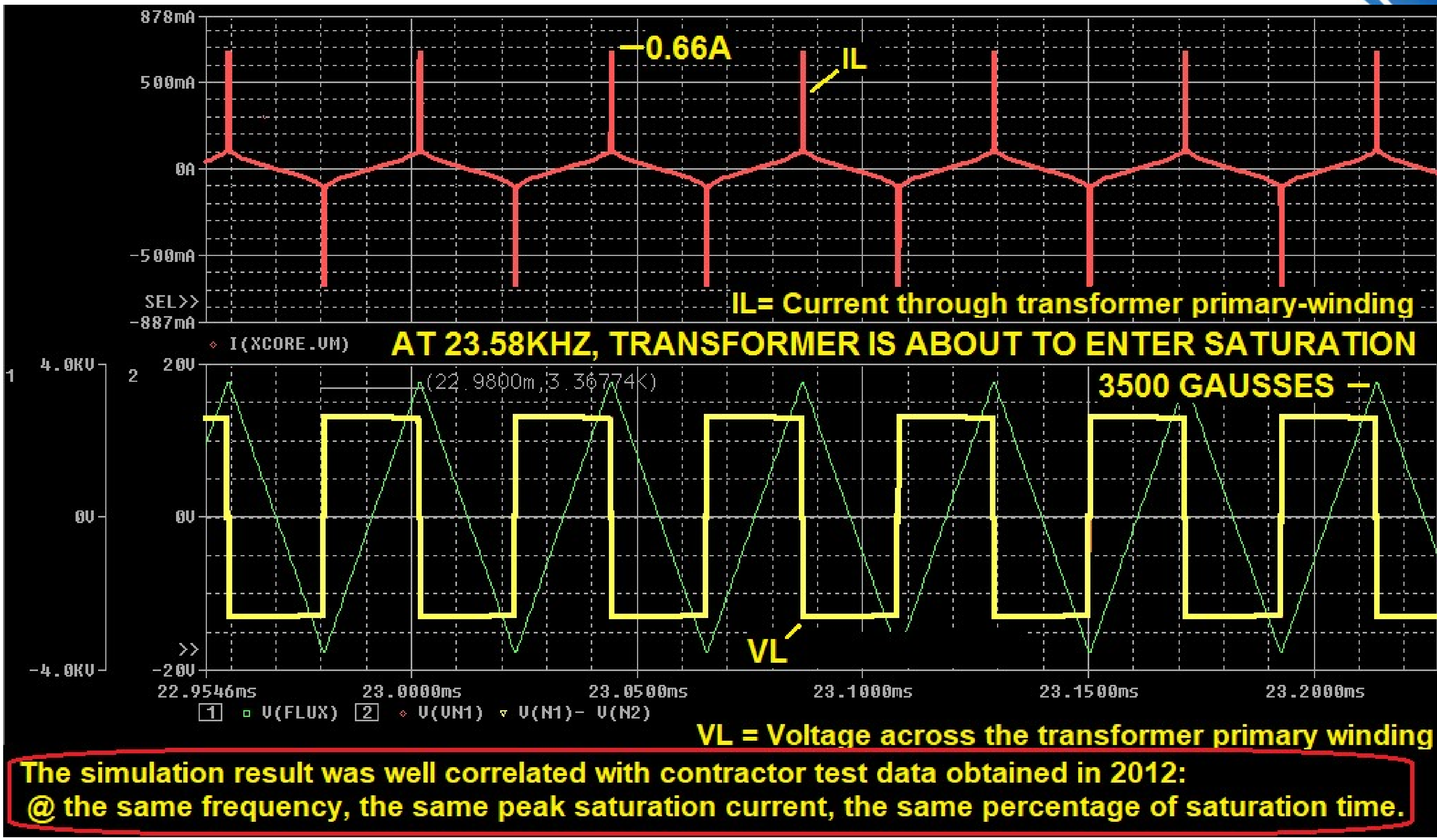

Magnetic saturation is observed from the saturated peak current spike of 0.66 A, which starts at around 23.58 kHz of transformer excitation frequency (square wave of +/-13 V amplitude) as PWM chip's temperature gets warmer.

Deep Magnetic Saturation due to Thermal Positive Feedback

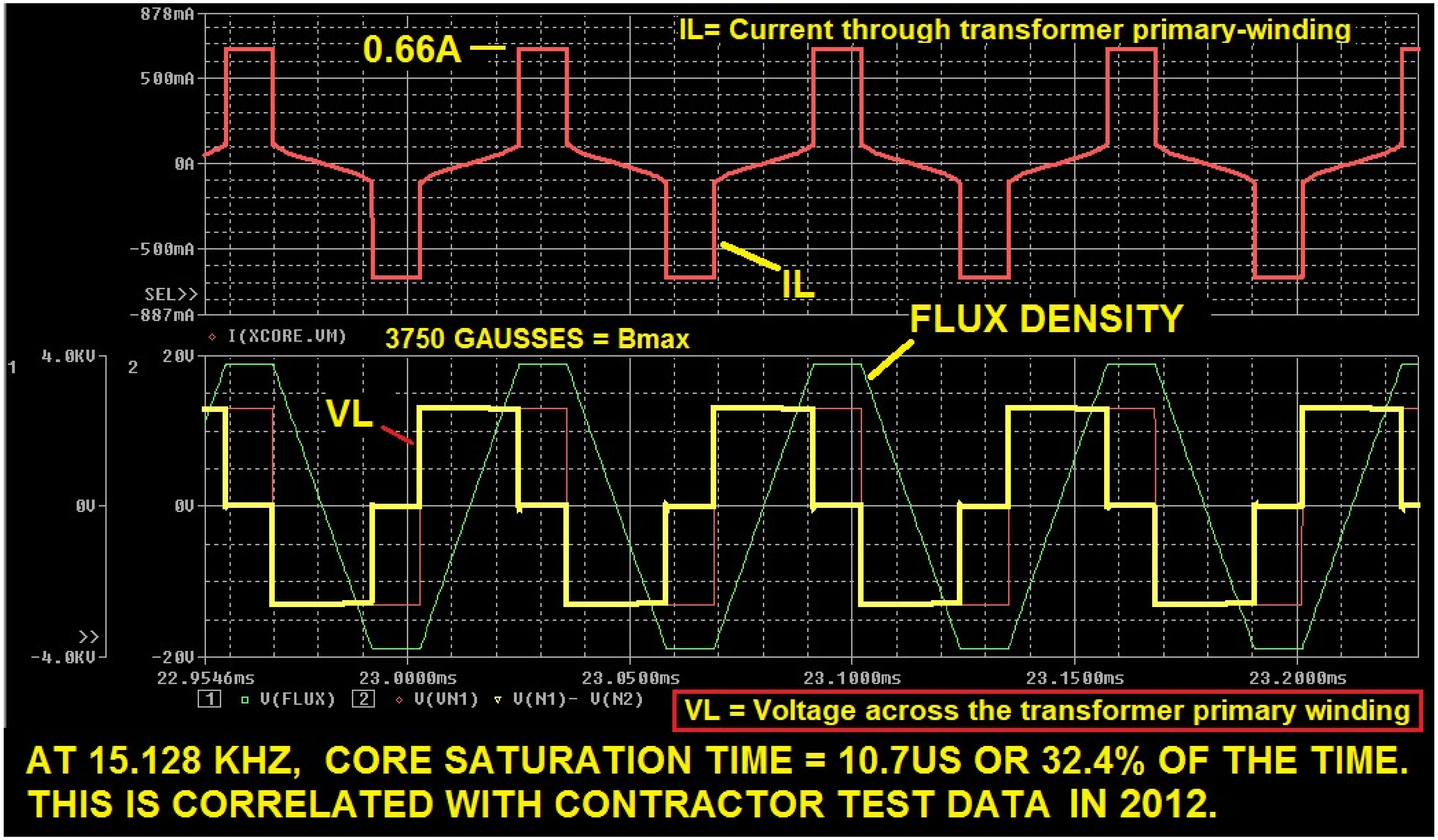

- PWM IC chip reduces the transformer operating frequency to 15.128 kHz, leading to deep saturation, which is well correlated with 2012 contractor test data